Postharvest Biology and Technology 211 (2024) 112804

Contents lists available at ScienceDirect

Postharvest Biology and Technology

journal homepage: www.elsevier.com/locate/postharvbio

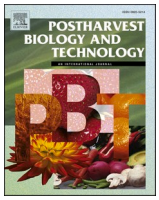

Bagging prevents russeting and decreases postharvest water loss of mango fruit cv. 'Apple'

Thomas O. Athoo [a], Dennis Yegon [b], Willis O. Owino [b], Moritz Knoche [a,*]

[a] Institute for Horticultural Production Systems, Leibniz-University Hannover, Herrenhäuser Straße 2, 30419 Hannover, Germany
[b] School of Food and Nutritional Sciences (SOFNUS), Jomo Kenyatta University of Agriculture and Technology, P.O. Box 62 000 – 00200, Nairobi, Kenya

ARTICLE INFO

Keywords:
Bag
Quality
Russet
Periderm
Lenticel
Cuticle
Transpiration
Permeance

ABSTRACT

In Kenya, the mango (*Mangifera indica* L) cultivar 'Apple' is commercially important but it often suffers excessive russeting, which both compromises its appearance and impairs its postharvest performance. Together, these effects seriously reduce its market potential. Exposure to surface moisture is implicated in russeting of cv. 'Apple' mango. The objective was to establish the effect of bagging on russeting. Developing fruit were bagged at the onset of the exponential growth phase, using brown paper bags (Blue star®). Un-bagged fruit served as controls. The brown paper bags were selected because of their high permeance to water vapor. At harvest maturity, bagged fruit were larger, less russeted and had smaller lenticels than un-bagged control fruit. Staining with aqueous acridine orange in conjunction with fluorescence microscopy revealed numerous microcracks and larger lenticels on un-bagged control fruit but these were not evident on bagged fruit. Postharvest mass loss (principally water loss) of bagged fruit was lower than of un-bagged control fruit. In the un-bagged control fruit, the skin's water permeance increased as the russeted surface area increased ($r^2 = 0.88$ **). Fruit skins were less permeable to water vapor than the brown paper bags. The brown paper bags contributed not more than 4.2 to 9.1% of the total in-series diffusion resistance of skin + bag. The masses of isolated cuticular membranes, and of dewaxed cuticular membranes, and of wax per unit surface area were higher for un-bagged control fruit than for bagged fruit. Bagged fruit were also greener and showed less blush. There was little difference in skin carotenoid content between bagged and un-bagged control fruit, but skin anthocyanin content was lower in bagged fruit. The rates of respiration and ethylene evolution of bagged fruit were lower than those of un-bagged control fruit. There were no differences between bagged and un-bagged control fruit in their organoleptic and nutritional properties including titratable acidity, total soluble sugars, sucrose, glucose, fructose, vitamin C and calcium content. In conclusion, bagging decreased russeting and increased postharvest performance of fruit of mango cv. 'Apple'.

1. Introduction

The mango cultivar 'Apple' is important in Kenya, where it is grown widely because of its excellent taste and textural properties. However, 'Apple' mango suffers from russeting. As a consequence, its appearance and postharvest performance are compromised. Russeted fruit is excluded from export to high-end markets, so russeting severely limits the market potential of this cultivar.

Russeting in 'Apple' mango occurs particularly in fruit from highland regions that are subject to extended periods of surface wetness (Athoo et al., 2020). To induce russeting for experimental purposes, deliberate exposure to surface wetness works well, especially during periods of most rapid growth (Athoo et al., 2022).

In botanical terms, 'russeting' refers to formation of a periderm and this is often triggered by rupture of the cuticle which in turn can be caused either by mechanical wounding or by microscopic cracking ('microcracking') (Faust and Shear, 1972, Winkler et al., 2022). As a consequence, a phellogen forms that divides and, to the outside, produces stacks of cork cells, the so called phellem (Evert, 2006). The cell walls of the phellem are impregnated with lignin and suberin (Evert, 2006) making them more waterproof and, so, partially restoring the barrier function previously exercised by the cuticle. The suberin is responsible for the brownish appearance of a russeted fruit surface and the irregular arrangement of the phellem cells for its dullness. Russeting is not unique to mango cv. 'Apple' but also occurs in a wide range of other fruit species including apple (*Malus domestica* Borkh.), pear (*Pyrus*

* Corresponding author.
E-mail address: moritz.knoche@obst.uni-hannover.de (M. Knoche).

https://doi.org/10.1016/j.postharvbio.2024.112804
Received 30 November 2023; Received in revised form 22 January 2024; Accepted 23 January 2024
Available online 2 February 2024
0925-5214/© 2024 The Author(s). Published by Elsevier B.V. This is an open access article under the CC BY license (http://creativecommons.org/licenses/by/4.0/).

communis L.), plum (*Prunus domestica* L.) and others (Faust and Shear, 1972; Skene, 1982; Michailides, 1991; Cohen et al., 2019; Shi et al., 2019; Winkler et al., 2022).

It is now well established that moisture on the fruit surface triggers microcracking of the strained cuticle in mango cv. 'Apple' (Athoo et al., 2022) and also in apples (Knoche and Grimm, 2008; Khanal et al., 2020), sweet cherries (Knoche and Peschel, 2006), and grapes (Becker and Knoche, 2012). The fruit cuticle is strained as a result of ongoing expansion growth. This stretches it as the underlying epidermal cells divide and extend (Knoche and Lang, 2017; Si et al., 2021). It has been shown that exposure to surface moisture alters the rheological properties of the cuticle in such a way as to increase the likelihood of failure (Edelmann et al., 2005; Khanal and Knoche, 2014, 2017). In 'Apple' mango, russeting is initiated close to lenticels (Athoo et al., 2020). These structures are stiffer than the general fruit surface and so serve to focus the growth stresses on the lenticel and its immediate vicinity (Brown and Considine, 1982; Considine, 1982). This fits with the observation that the lenticels in an area of moisture-exposed fruit skin are markedly larger than those in a similar but un-exposed area (Athoo et al., 2023).

At present, there are no agronomic strategies for russeting prevention or mitigation in mango cv. 'Apple'. Due to the known role of surface moisture in exacerbating russeting, it is hypothesized that bagging of fruit at the beginning of the period of most rapid surface expansion growth will shorten the duration of surface wetness or even prevent it entirely. This being the case, cuticular microcracking will be reduced or prevented and thus russeting. Comparable effects have been reported for pear (Amarante et al., 2002; Lin et al., 2008) and *Malus* apples (Tukey, 1969; Moon et al., 2016; Yuan et al., 2019). Bagging reduced lenticel discoloration in mango cv. 'Apple' (Mathooko et al., 2011).

The objective of this study was to determine the effect of bagging developing fruit of mango cv. 'Apple' on russeting and postharvest performance.

2. Materials and methods

2.1. Plant materials

Fruit of mango (*Mangifera indica* L.) cv 'Apple' grafted on seedling rootstocks was obtained from commercial orchards located in Kaiti (1°45′S, 37°28′E) and Kambirwa (0°44′S, 37°12′E), Kenya. Unless otherwise specified, fruit were harvested at commercial maturity based on raised shoulders and fullness of the cheeks and freedom from visual defects. Fruit were examined within 48 h of harvest.

2.2. Experiments

2.2.1. Selecting the bags

We investigated the water vapor permeance (m s^{-1}) and light absorption characteristics (A) of a brown paper bag (Blue star; King Plastic Industries, Nairobi, Kenya), a waxed white paper bag (Majimaji; King Plastic Industries) and a single layered white paper bag with clamping wire (G-26; Kobayashi Bag Manufacturing Company, Lida, Japan). We will refer to these as 'brown paper bag', 'waxy white paper bag' and 'white paper bag', respectively (See supplementary Fig. S1 for illustration).

To determine the permeance of the bags to water vapor, paper discs (15 mm in diameter) were punched from the bags and mounted in custom-made stainless steel diffusion cells (Geyer and Schönherr, 1988; Knoche et al., 2000) using high-vacuum grease. The gap between the lid and the bottom of the diffusion cell was sealed using clear transparent adhesive tape (Tesa Film®; Tesa-Werke Offenburg, Offenburg, Germany). Deionized water was injected into the cells through an orifice in the lower part using a disposable syringe and the orifice subsequently tape sealed. The cells were turned upside down and left overnight to equilibrate under ambient conditions. The cells were then placed in a sealed polyethylene (PE) box containing dry silica gel, such that the exposed bag surface in the diffusion cell faced the silica gel. The diffusion cells were weighed at 2 h intervals for up to 8 h. The rate of water loss (F, g h^{-1}) was calculated from the slope of a linear regression fitted through a plot of diffusion cell mass (kg) against time (h). The average r^2 was usually better than 0.99. The permeance (P, m s^{-1}) of the bag was then calculated using Eq. 1 (Nobel, 2020).

$$P = \frac{F}{A \times \Delta C} \quad (1)$$

In this equation, A is the exposed area of the diffusion cell

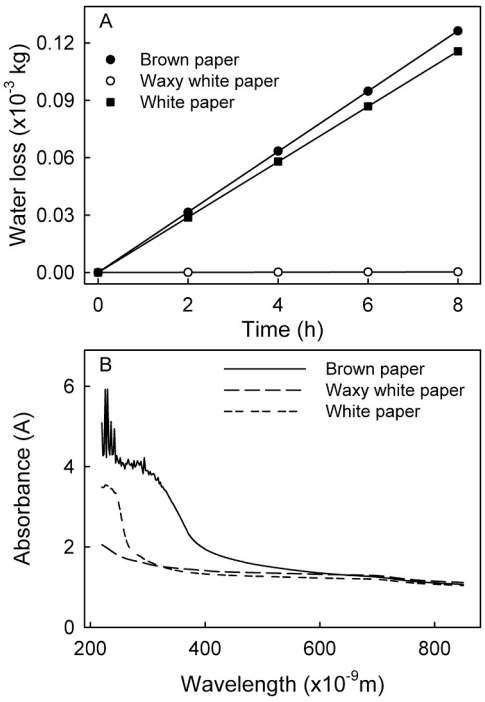

Fig. 1. (A) Cumulative water loss through samples of different bagging materials with time. The patches were mounted inside custom made diffusion cells and incubated above dry silica inside a polyethylene box. The bags were made of brown paper, waxy white paper and white paper. The number of replicates was 20. (B) Light absorbed by different bag materials at wavelengths between 220–850 × 10^{-9} m was measured using a photometer. A single layer of bag material was mounted on a cuvette for the absorbance measurement, an empty cuvette was measured for reference. The bags were made of brown paper or waxy white paper or white paper. The number of individual replicates was three.

Table 1
Resistances and relative contributions of bagging material to total resistance to water vapor loss from bagged cv. 'Apple' mango. The bagging materials were brown paper, waxy white paper and white paper bags. Resistance was calculated as the inverse of permeance (m s^{-1}). Permeance was calculated from the rate of cumulative water loss vs time through samples of the bag materials mounted in diffusion cells (see supplementary Fig. 1). The number of replicates was 20.

Bagging material	Resistance bag (s m^{-1})	Total resistance (Skin +bag)		Contribution of bag to total resistance (%)	
		min	max	min	max
Brown paper bag	181	1995	4320	9.1	4.2
Waxy white paper bag	69341	71156	73480	97.5	94.4
White paper bag	197	2011	4336	9.8	4.5

The minimum (1814 s m^{-1}) and maximum resistances (4139 s m^{-1}) of the fruit skin were calculated as the inverse of the permeances of a non russeted fruit (russet score 0 = 0% russeted area) and a russeted fruit skin (russet score 4 = 51-100% russeted area) from the regression line in Fig. 4.

Table 2
Photosynthetically active radiation (PAR) and percentage PAR absorption of the three different bagging materials. Measurements were made on in full sunlight and a bright sky. Control was measurement without any bagging material. The number of replicates was three. Data represent means ± se.

Fruit bag	PAR (μmol s^{-1} m^{-2})	PAR absorbed (%)
None (Control)	2022.7 ± 0.3	0.0
Waxy white paper	1325.7 ± 11.2	34.5
Brown paper	595.7 ± 1.8	70.6
White paper	1416.0 ± 17.6	30.0

(3.85×10^{-5} m^2) and ΔC the difference in water vapor concentration between the water vapor saturated atmosphere inside the diffusion cell (20.59 g m^{-3} at 23 °C) and the dry environment inside the PE box (approximately 0 g m^{-3} at 23 °C) (Nobel, 2020). The resistance (R; s m^{-1}) was calculated as the inverse of permeance. The number of replicates was 20 per bag.

Cumulative water vapor loss through the different bagging materials increased linearly with time indicating a constant permeance to water vapor (Fig. 1 A). The resistance to water vapor movement was highest for the waxy white paper bag and markedly lower for both the white paper bag and the brown paper bag (Table 1).

The light absorbance (A) of the bags was determined by photometry. A piece of the bag was mounted on the surface of a semi-micro UV cuvette (Brand 759150; Brand GmbH + CO KG, Wertheim, Germany). Absorbance (wavelength, m) was recorded in 2.20×10^{-7} m steps between 2.2 and 8.5×10^{-7} m using a spectrophotometer (Specord 210; Analytik Jena GmbH, Jena, Germany). An empty cuvette without a bag sample served as control.

The waxy white paper bag and the white paper bag absorbed less light compared with the brown paper bag (Fig. 1B). Most of the absorption occurred in the range of short wavelengths. There was less absorption at wave lengths above 4.0×10^{-7} m with little difference between the different bags.

The photosynthetic active radiation (PAR) absorbed by the bags was measured in full sunlight using a LI-250 light meter fitted with a quantum sensor (LI-COR Biosciences GmbH, Bad Homburg, Germany). The sensor was either left uncovered to face the sun (control) or covered by a single layer of the bagging material. The PAR absorbance of the bags was expressed as a percent fraction of the PAR reading by the uncovered light sensor. The number of replicates was three.

The waxy white paper bag and the white paper bag also absorbed less PAR compared with the brown paper bag (Table 2).

Based on these data and local availability, the brown paper bags were selected for the bagging experiment.

Fruit were bagged at 59 days after full bloom (DAFB) at Kambirwa and at 60 DAFB at Kaiti. This timing corresponded to the onset of the exponential growth phase at the two sites. The open end of the bag was tied to the peduncle using a fine wire. A small hole (1 cm^2) was cut at the bottom of the bag to drain away any free water that may have entered the bag along the peduncle. The bags were left attached to the fruit until maturity; un-bagged fruit served as controls.

2.2.2. Developmental time course in fruit growth and cuticle deposition

The developmental time course of change in fruit mass, surface area and cuticle deposition were established. Fruit mass (kg) was determined by weighing (TX420L; Shimadzu Corporation, Kyoto, Japan). Fruit length (m) and the two orthogonal diameters (m) recorded at the equatorial plane were measured using a digital caliper (CD-20PKX; Mitutoyo, Kawasaki/Kanagawa, Japan). Fruit surface area (m^2) was calculated from the measured dimensions assuming a spherical shape. An earlier study established that the calculated and measured surface areas using excised peels are closely related: $Calculated\ area(spheroid) = 0.93 + 1.18(\pm 0.04) \times measured\ peel\ area, r^2 = 0.98^{**}$ (Athoo et al., 2021). A sigmoid regression curve was fitted through a plot of fruit surface area against time. The growth rate (m^2 d^{-1}) was calculated as the first derivative of the model. The number of individual fruit replicates was 30.

To quantify cuticle deposition, skin segments (ES) were excised from the cheek using a biopsy punch (8 mm diameter; Kai Europe, Solingen, Germany). The ES were incubated in 50 mM citric acid buffer solution containing cellulase (5 mL L^{-1}; Cellubrix L; Novozymes A/S), pectinase (90 mL L^{-1}; Panzym Super E flüssig; Novozymes A/S, Krogshoejvej, Bagsvaerd, Denmark) and 30 mM sodium azide to prevent bacterial growth (Orgell, 1955). The pH was adjusted to pH 4.0 using NaOH. The solution was refreshed periodically until the cuticle separated from the adhering tissues. The isolated cuticles were cleaned using a soft, camelhair brush. Following thorough rinsing with deionized water, the cuticular membranes (CM) were dried overnight at 40 °C and then weighed (CPA2P; Sartorius AG, Göttingen, Germany). The CM were Soxhlet extracted for 2 h to remove cuticular wax using a chloroform: methanol mix (1:1 v:v $CHCl_3$:MeOH). The dewaxed CM (DCM) were dried overnight at 40 °C and then re-weighed (CPA2P; Sartorius). The masses per unit area of the CM, DCM and wax (kg m^{-2}) were calculated. The number of CMs processed at each sampling time was 20.

2.2.3. Fresh mass and russeting

Mature fruit were harvested at 117 DAFB at Kaiti and at 126 DAFB at Kambirwa. Fresh mass (Kg) was recorded (TX420L, Shimadzu). Russeting was quantified using a discontinuous five-step rating scheme (Athoo et al., 2020). The ratings were: score 0 = 0% of the fruit surface area russeted, score 1 = 1–10% of the surface area russeted, score 2 = 11–25% of the area russeted, score 3 = 26–50% of the area russeted and score 4 = >51% of the area russeted. An earlier study had established that these rating scores were closely correlated to russeted surface area as measured by digital photography and image analysis.

$Russeted\ area(rating\ score) = \sqrt{(0.23(\pm 0.01) \times measured\ area(\%)}$, $r^2 = 0.96^{***}$) (Athoo et al., 2020). The number of individual fruit replicates was 135 for Kaiti and 193 for Kambirwa.

2.2.4. Lenticel size

The effect of bagging on lenticel size was determined at maturity. Briefly, ES were excised from the fruit cheek using a biopsy punch (8 mm diameter; Kai Europe, Solingen, Germany). The ES were viewed under a stereo microscope (MZ10F; Leica Microsystems, Wetzlar, Germany) and photographed (Camera DFC7000T; Leica Microsystems). The core area and the pore area of each lenticel (mm^2) were quantified by image analysis (ImageJ 1.53 P; National Health Institute, Bethesda, MD, USA). Here, we refer to the entire subepidermal lenticel as the 'core' and the open, cracked area of the lenticel as the 'pore'. The number of individual fruit replicates was 25.

2.2.5. Microcracking of the cuticle

To study the effect of bagging on formation of microscopic cuticular cracks (microcracks), bagged and un-bagged control fruit were dipped in 0.1% aqueous acridine orange solution for 10 min (Peschel and Knoche, 2005). Aqueous acridine orange penetrates the epidermal layer through a microcrack in the cuticle surface but not through the intact cuticle. Following rinsing with distilled water, the fruit surface was inspected for microcracks under a stereo microscope (MZ10F; Leica Microsystems) in brightfield and fluorescing light (GFP LP filter, 480–440 nm excitation, ≥510 nm emission wavelength). Calibrated images were taken with a digital camera (Camera DFC7000T; Leica Microsystems). The number of individual fruit replicates was five.

2.2.6. Postharvest water loss

The effect of bagging on postharvest water loss was investigated. Bagged and un-bagged control fruit were rated individually for russeting. Fruit mass, and orthogonal dimensions were determined and the fruit surface area (m^2) calculated.

The time course of transpiration was established on a whole-fruit basis (kg). Transpiration was restricted to the skin by sealing the stem end using a fast-curing silicone rubber (Dow Corning SE 9186; Dow Corning Corp, Midland, MI, USA). After a minimum curing period of 20 min, fruit were placed in a polyethylene (PE) box containing a saturated solution of NaCl (relative humidity 75%) (Wexler, 1995). Under these conditions the difference in water vapor concentration across the fruit skin was 4.67 g m^{-3} (Wexler, 1995). Fruit were weighed individually every 24 h for up to 96 h. The rate of water loss, the permeance and the resistance were calculated as described above. The number of individual fruit replications was 20.

From the permeance estimates of the bag, of the russeted and the unrusseted fruit skins, the relative contributions of the bag to total resistance (bag + skin) were calculated using a 'resistors-in-series' model according to the following equations (Nobel, 2020):

$$R = \frac{1}{P} \tag{2}$$

$$R_{tot} = R_{bag} + R_{skin} \tag{3}$$

In this equation resistance (R; s m^{-1}) equals the inverse of the permeance (P; m s^{-1}) and total resistance of bag plus skin (R_{tot}) equals the some of the resistance of the bag (R_{bag}) plus that of the skin (R_{skin}) in analogy to resistors arranged in series in an electrical circuit (Nobel, 2020).

2.2.7. Peel color

Peel color was quantified in the CIE LAB 1976 (L*, a*, b*) color space using a spectrophotometer (CM-23D, 8 mm orifice; Konica Minolta, Osaka, Japan; software: SpectraMagic™ NX Professional/Lite v 3.3). A total of four fruit were measured, making four measurements per fruit. Hue angles (°) were calculated from the a* and b* values according to McGuire (1992).

2.2.8. Carotenoids and anthocyanins

Whole fruit were peeled and the peel stored at − 18 °C until use. Following thawing, adhering flesh was removed from the peel by gentle scraping, to leave just the epidermis and hypodermis. The peel was then chopped into small fragments. To quantify carotenoids, a sample of 3 g of peel was ground in 10 mL acetone in a mortar. The resulting acetone extract was then transferred to a 50 mL volumetric flask. The peel was extracted several times until the extracts were colorless. The extracts were combined and brought up to 50 mL volume using acetone. Petroleum ether (30 mL) was added to a separation funnel followed by the acetone extract. Distilled water was then added to remove the acetone. The procedure was repeated three times, the extracts were combined and brought up to 50 mL volume by adding petroleum ether. Absorbance of the extract was determined at 450 nm using a UV-Vis spectrophotometer (UV-1800 spectrophotometer, Shimadzu) (Heinonen, 1990; Rodriguez-Amaya and Kimura, 2004). Carotenoid content was calculated from Eq. 4 (Rodriguez-Amaya and Kimura, 2004).

$$Carotenoids = \frac{A \times V \times 10^4}{A^{1\%}_{1cm} \times Sample \quad weight} x100 \tag{4}$$

In this equation A is the absorbance of the extract read at 450 nm, V (mL) the volume of the extract and $A^{1\%}_{1cm}$ the absorbance coefficient of β-carotene in petroleum ether (Rodriguez-Amaya and Kimura, 2004). Results are given on a fresh weight basis (g kg^{-1}). The number of individual fruit replicates was three.

Anthocyanins were determined using the pH differential method (Lee et al.,2005). Briefly, 3 g of peel was ground in a mortar, then extracted in 10 mL of methanol for 72 h on a shaker, in the dark. The extract was divided into two aliquots. The first was buffered in 25 mM KCl buffer at pH 1.0. The second was buffered in 400 mM Na-acetate buffer at pH 4.5. The pH was adjusted to 1.0 or 4.5 using HCl. Solutions were filtered (filter paper grade 1; cut-off pore size 11 μm) to remove any particulate matter (turbidity). Absorbance of the filtrate was measured at 520 and 700 nm within 20–50 min of preparation of the extracts using a spectrophotometer (UV-1800; Shimadzu). The anthocyanin pigment concentration was calculated as cyanidin-3-glucoside equivalents using Eq. 5 (Lee et al.,2005).

$$Anthocyanin = \frac{A \times MW \times DF \times 10^3}{\varepsilon \times l} \tag{5}$$

and

$$A = \left(A^{ph1}_{520} - A^{ph1}_{700}\right) - \left(A^{ph4.5}_{520} - A^{ph4.5}_{700}\right)$$

In this equation A is the differential absorbance of the buffered extracts at pH 1.0 and 520 nm (A^{pH1}_{520}), pH 1.0 and 700 nm (A^{pH1}_{700}), at pH 4.5 and 520 nm ($A^{pH4.5}_{520}$) and at pH 4.5 and 700 nm ($A^{pH4.5}_{700}$), MW the molar mass of cyanide-3-glucoside (449.2 g mol^{-1}), DF is the dilution factor, ε the molar extinction co-efficient (26900 L mol^{-1} cm^{-1}) of cyanidin-3-glucoside and l is the path length of the beam through the extract (cm) (Lee et al.,2005). Results are given on a fresh weight basis (g kg^{-1}). The number of individual fruit replicates was three.

2.2.9. Respiration and ethylene synthesis

Rates of respiration and ethylene synthesis were determined during shelf life at ≈ 25 °C for up to 15 d after harvest (DAH) with three to six individual fruit replicates.

The rate of respiration was estimated as the rate of CO_2 production per unit fruit mass. Fruit were individually incubated in gastight plastic jars (volume 2 L) for 1–1.5 h at ambient temperature (23–25 °C). A gas sample (1 mL) was drawn from the headspace using a gastight syringe and injected into a gas chromatograph. The CO_2 concentration was determined using a GC (GC-8A; Shimadzu) equipped with a Porapack Q column and a thermal conductivity detector. The injector temperature was 150 °C, the column and detector temperatures 120 °C. Helium was used as a carrier gas at a flow rate of 20 mL min^{-1}. The rate of CO_2 production (μg kg^{-1} s^{-1}) was calculated from the increase in CO_2 concentration in the incubation jar during the incubation interval.

Ethylene was quantified on a GC (GC-9A; Shimadzu) equipped with an activated alumina column (Sepax HP- Amino, 5 μL; Sepax™ Technologies Inc, Newark, DE, USA) and a flame ionization detector. The injector temperature was set at 220 °C, the column temperature at 150 °C, and the detector temperature at 240 °C. The carrier gas was N_2 at a flow rate of 50 mL min^{-1}. Hydrogen and synthetic air were used as the burning gas for the detector at flow rates of 50 mL min^{-1} for H_2 and 5 mL min^{-1} for synthetic air. The rate of ethylene evolution was calculated (ng kg^{-1} s^{-1}) from the increase in ethylene concentration during the incubation interval. Calibration curves were established to calculate CO_2 and ethylene concentrations from the respective peak areas.

2.2.10. Firmness

Fruit firmness (N) was measured during shelf life, before and after peeling, using a rheometer (probe diameter 5 mm) (Compac-100; Sun scientific, Tokyo, Japan). The distance of travel was set at 20 mm and the travel speed adjusted to 600 mm min^{-1}. The number of individual fruit replicates ranged from 12 to 16.

2.2.11. Total acidity and total soluble solids

Pulp samples were prepared from fruit flesh using a blender. Briefly, 5 g of pulp was added to 50 mL of distilled water. The indicator phenolphthalein (40–60 μL) was added to a 10 mL aliquot of the solution and titrated against 0.1 N NaOH until color change. From the volume of base consumed, total acidity (TA) was calculated as the percent (%) of citric acid equivalent according to ISO 750:1998 (factor for citric acid 0.064;(ISO, 1998)). Total soluble solids (TSS, %) of the pulp were determined using a digital refractometer (PAL-S; Atago, Tokyo, Japan). The number of individual fruit replicates was three.

2.2.12. Sucrose, glucose and fructose

The sucrose, glucose and fructose contents of the pulp (g kg^{-1}) of bagged and un-bagged control fruit was quantified during shelf life using the method described by Li (1996). About 2 g of pulp was boiled in 20 mL of ethanol for 1 h inside a reflux condenser (SF-6, Sanshin Industrial Co, Kobe, Japan). Upon cooling, the extract was filtered, and the solvent evaporated from the filtrate in a rotary evaporator (DGU-20A 5 R, Shimadzu). The residue was taken up in 5 mL of acetonitrile and water (1:1 v/v). An aliquot (1 mL) of supernatant was micro-filtered (Nylon syringe filter, pore size 0.45 μm; Membrane Solutions LLC, Auburn, WA, USA) into a vial. Sucrose, glucose and fructose were analyzed by high-performance liquid chromatography (HPLC) (LC-20AD; Shimadzu) fitted with a refractive index (RI) detector (model 10 A, Shimadzu). The HPLC was run using the following settings: oven temperature 30 °C, injection volume 20 μL, mobile phase acetonitrile: water (75:25) at 0.5–1.0 mL min^{-1}. Calibration lines were established using standards. Total sugars were calculated as the sum of glucose, fructose and sucrose. Results are given on a fresh weight basis (g kg^{-1}). The number of individual fruit replicates was three.

2.2.13. Vitamin C

The change in ascorbic acid content during shelf life was analyzed by HPLC using the procedure of Vikram et al. (2005). About 2.5 g of pulp was weighed and dissolved in 0.8% metaphosphoric acid. The solution was then centrifuged for 10 min at 11739 g and 40 °C. The supernatant was filtered through a 0.45 μm filter (Nylon syringe filter; Membrane Solutions LLC). A 20 μL sample of the filtrate was injected into an HPLC (Model 20 A; Shimadzu) equipped with a UV- Vis detector (SPD 20 A; Shimadzu). Absorbance was read at 266 nm. The settings of the HPLC were: oven temperature 30 °C and flow rate of 1.2 mL min^{-1}. Metaphosphoric acid (0.8%) was also used as a solvent. This acid was vacuum-filtered (Rocker-Chemker 300; Rocker Scientific, New Taipei, Taiwan) and degassed using an ultrasonic cleaner (GT sonic 3; GT International (HK) Group, Shenzhen, China).

A calibration curve was prepared using ascorbic acid standards in a concentration range from 10 to 100 mg L^{-1}. Results are given on a fresh weight basis (g kg^{-1}). The number of individual fruit replicates was three.

2.2.14. Calcium

Because Ca in the flesh is implicated to play a role in physiological disorders such as soft-nose (Burdon et al., 1991) and spongy tissue (Ma et al., 2023) and because bagging could affect fruit transpiration which - in turn – is the driving force for Ca import into the fruit, we determined the Ca content of the flesh. Calcium content was analyzed by spectrophotometry following dry ashing (Isaac and Johnson, 1975; Osborne and Voogt, 1978). Briefly, 5 g of pulp was placed into a pre-weighed crucible. The sample was ashed in a muffle furnace (Advantec KL-420; Electric Muffle furnace, Toyo Seisakusho Kaisha, Chiba, Japan). The temperature of the furnace was increased to 550 °C, held constant for 1 h and decreased thereafter. The ash was taken up in 20 mL of 0.5 N HNO_3, then heated to 80–90 °C on a hotplate for 5 min and brought up to 100 mL volume using 0.5 N HNO_3. The solution was filtered (filter paper grade 1; cut-off pore size 11 μm). Lanthanum chloride (0.5 mL at 0.12 M) and distilled water (9 mL) were added to 0.5 mL of sample to make the test solution. Absorbance of the solution was read using an atomic absorption spectrophotometer (Model AA-7000 with ASC-7000 Auto sampler; Shimadzu). A calibration curve was prepared prior to analysis. Results are given on a fresh weight basis (g kg^{-1}). The number of individual fruit replicates was three.

2.3. Data analysis, statistics and terminology

Data are presented as means ± se. Where not visible, the standard error bars were smaller than the data symbols. Data were analyzed using analysis of variance with R statistical software (R version 4.0.3; R Foundation for Statistical Computing, Vienna, Austria). Means were separated using Tukey's studentized range test ($\alpha = 0.05$). Regression analyses were conducted in R and Sigma Plot (version 12.5; Systat Software, San Jose, CA, USA). We refer to microcracking of the cuticle that is associated with lenticels as 'lenticel cracking'.

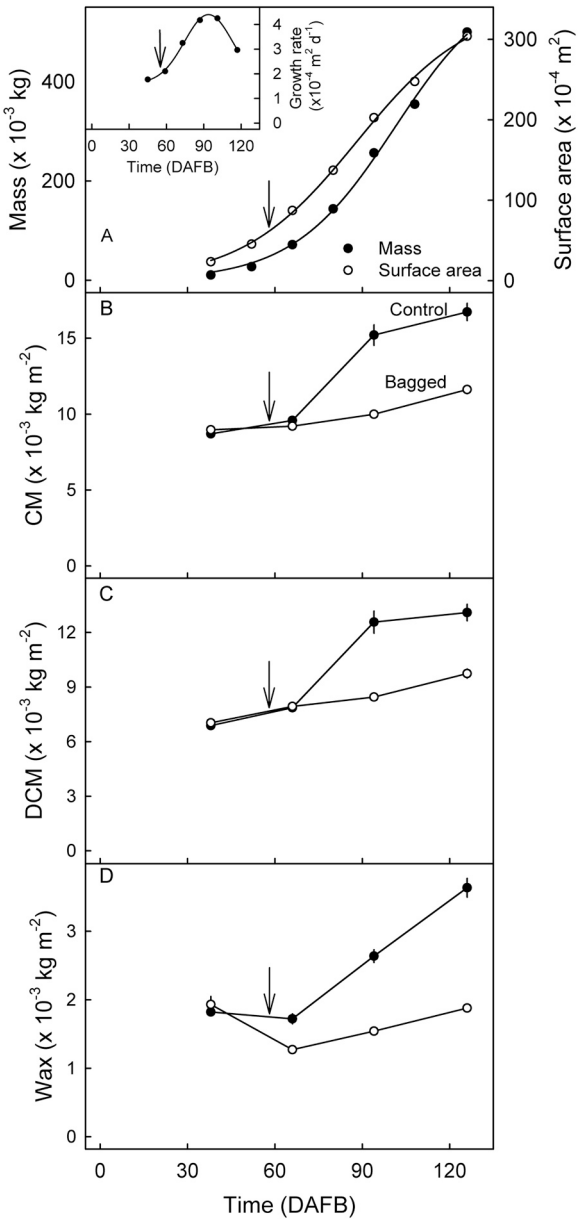

Fig. 2. Developmental time course of change in fruit mass and surface area (A) and surface area growth rate (A, inset), deposition of the cuticular membrane (CM) (B), the dewaxed CM (DCM) (C) and wax of 'Apple' mango. Vertical arrows indicate the time at which the fruit were bagged at Kambirwa using brown paper bags. Un-bagged fruit served as controls. X-axis scale in days after full bloom (DAFB). Data represent means ± se. The number of replicates was 30 in A, and 20 in B, C, and D.

3. Results

Fruit mass and surface area increased sigmoidally with time. Surface area growth rate reached a maximum of 4.3×10^{-2} m^2 d^{-1} at 94 DAFB (Fig. 2A). The mass of CM, DCM and wax per unit surface area all increased during development. The CM, DCM and wax mass were significantly higher for the un-bagged control fruit than for the bagged

Table 3
Average (means ± SE) fruit mass of bagged and un-bagged control 'Apple' mango. The fruit were bagged at 59 days after full bloom (DAFB) in Kambirwa and at 60 DAFB in Kaiti using brown paper bags. Un-bagged fruit served as controls. The number of replicates was 193 in Kambirwa and 135 in Kaiti.

Treatment	Mass (x 10^{-3} kg)		
	Kaiti	Kambirwa	Mean $_{Treatment}$
Control	371.7 ± 9.0	313.5 ± 7.0	342.6 ± 5.8 a^{y}
Bagged	424.4 ± 8.9	348.8 ± 5.8	386.6 ± 5.4 b
Mean $_{Site}$	398.0 ± 6.5 b^{z}	331.2 ± 4.6 a	

Main effect of treatment ^{y} and orchard site ^{z} but not interaction significant following two factorial ANOVA at $P \leq 0.05$. Mean separation by Tukey's Studentized Range test, $P \leq 0.05$

fruit (Fig. 2B-D).

At maturity, the mass of the bagged fruit exceeded that of the un-bagged control fruit (Table 3). Fruit grown in Kaiti, was consistently larger than that from Kambirwa (Table 3).

Bagged fruit were less russeted and had markedly smaller lenticels than those of un-bagged control fruit (Fig. 3, Tables 4,5). There were no significant differences in russeting or in lenticel size between fruit from Kaiti or Kambirwa (Tables 4,5).

Fluorescence microscopy revealed numerous dye infiltrated microcracks and lenticels on the surface of un-bagged control fruit, but there were no microcracks or infiltrated lenticels on the surface of bagged fruit (Fig. 3).

Simulated postharvest mass loss from bagged and un-bagged control fruit increased linearly with time (Fig. 4 A,B). Mass loss (mostly water loss) and skin permeance were about 1.8-fold higher in un-bagged control fruit, compared with fruit that had been bagged (Fig. 4B). For control fruit, permeance was positively and linearly related to the area of surface russeted ($r^2 = 0.88$ **) (Fig. 4C). Compared to the bag material, fruit skins were markedly less permeable and thus had a much higher resistance to water vapor loss than either the brown paper bag or the white paper bag (Table 1). Consequently, the brown paper bag and the white paper bag contributed to at most only 4.2% and 4.5%, respectively, to the maximum total resistance. This result contrasted with that with the waxy white bag, which contributed up to 94.4% to the maximum total resistance (Table 1). Thus, the relative humidity inside

Table 4
Average (mean± se) russeting in bagged and un-bagged control 'Apple' mango from Kaiti and Kambirwa production sites. The fruit were bagged at 59 days after full bloom (DAFB) in Kambirwa and at 60 DAFB in Kaiti using brown paper bags. Un-bagged fruit served as controls. Russeting was quantified using a five-score rating scheme. Score 0 = 0% of the fruit surface area russeted, Score 1 = 1–10% russeted area, score 2 = 11–25% russeted area, score 3 = 26–50% russeted area and score 4 = 51–100% russeted area. The number of replicates was 193 in Kambirwa and 135 in Kaiti.

Treatment	Russeting (rating)		
	Kaiti	Kambirwa	Mean $_{Site}$
Control	1.8 ± 0.1 b^{z}	2.3 ± 0.1 b	2.1 ± 0.1
Bagged	0.2 ± 0.0 a	0.2 ± 0.0 a	0.2 ± 0.0
Mean $_{treatment}$	1.0 ± 0.0	1.3 ± 0.1	

z Interaction treatment x site significant by two factorial ANOVA. Therefore, ANOVA run by sites. Means within the rows followed by the same letter are not significantly different. Mean separation by Tukey studentized range test, $P \leq 0.05$

Table 5
Pore (opening) and core (underlying cavity) area of lenticels in bagged and un-bagged control mature 'Apple' mango. The fruit were bagged at 59 days after full bloom (DAFB) in Kambirwa and at 60 DAFB in Kaiti using brown paper bags. Un-bagged fruit served as controls. The number of replicates was 193 in Kambirwa and 135 in Kaiti.

Treatment	Lenticel area (mm^2)			
	Kaiti		Kambirwa	
	Pore area	Core area	Pore area	Core area
Control	0.39 ± 05 b^{z}	0.95 ± 0.13 b	0.35 ± 05 b	0.95 ± 0.13 b
Bagged	0.01 ± 00 a	0.05 ± 0.01 a	0.00 ± 00 a	0.04 ± 0.01 a

z Main effect treatment significant by two factorial ANOVA. Mean separation according to the Tukey Studentized Range test, $p \leq 0.05$.

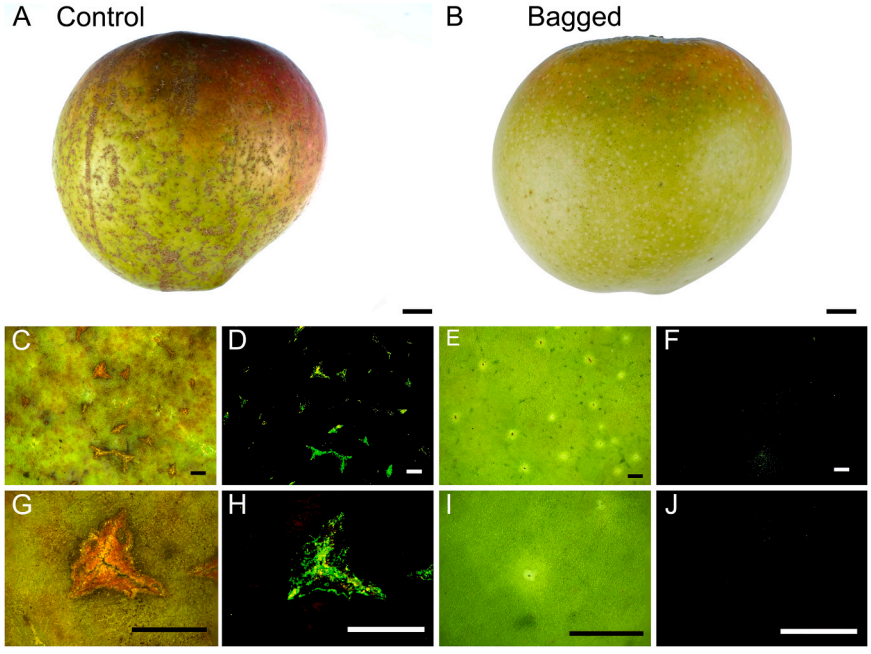

Fig. 3. Representative images of un-bagged ('Control') (A) and bagged ('Bagged') (B) 'Apple' mango at maturity. Microscopic view of fruit surface (C-E) and lenticels (G-J) of un-bagged (C,D,G,H) and bagged (E,F,I,J) 'Apple' mango at harvest. Fruit were viewed under incident bright (C,E,G,I) or under incident fluorescent light to visualize microcracks (D,F,H,J). Areas of the fruit surface were incubated in 0.1% aqueous acridine orange prior to microscopy. Scale bar is 1 cm (A,B) and 1 mm (C-E). The number of replicates was five.

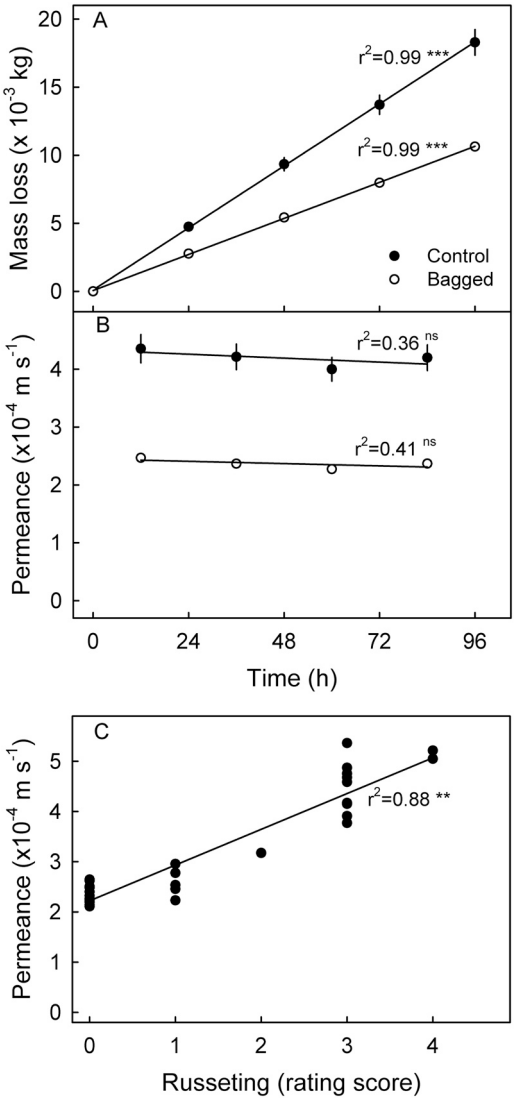

Fig. 4. Time course of fruit mass loss (A) and change in permeance (B) of mature 'Apple' mango. The fruit were either bagged ('Bagged') or remained un-bagged ('Control') at Kambirwa at 59 days after full bloom. Data represent means ± se. (C) Relationship between the permeance of the fruit skin to water vapor and the portion of the fruit surface area russeted. Russeting was quantified using a five-point scoring scheme. Score 0 = 0% of the fruit surface area russeted, Score 1 = 1–10% russeted area, score 2 = 11–25% russeted area, score 3 = 26–50% russeted area and score 4 = 51–100% russeted area. Data in C represent individual fruits. The number of individual fruit replicates was 15. The regression equation was: $Permeance(\times 10^{-4}\ \ m^{-1}) = 2.22(\pm 0.1) + 0.71(\pm 0.1) \times russet\ score$, $r^2 = 0.88$ * *.

the bags would have been markedly higher in the waxy white bags as compared with either the brown paper bag or the white paper bag.

Bagged fruit were greener and had less blush on the surface than un-bagged control fruit, as indexed by a lower hue angle (Fig. 5). The hue angle decreased during ripening, indicating de-greening. This change was in part due to an increase in total carotenoids as the fruit ripened (Fig. 5B,C). There was no significant difference in carotene content between bagged and un-bagged control fruit. Anthocyanin content increased with ripening and was consistently higher for un-bagged control fruit compared with for bagged fruit (Fig. 5D).

The rates of respiration, as indexed by CO_2 release, increased with ripening, peaked at about 10 days after harvest (DAH) and then declined. The respiration rate of un-bagged control fruit exceeded that of bagged fruit by up to 1.4-fold. A similar pattern was observed for

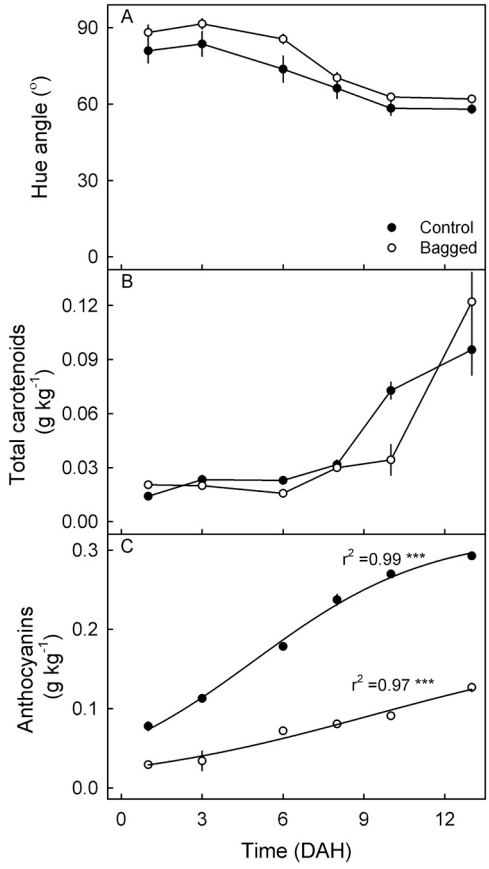

Fig. 5. Hue angle (A), carotenoid (B), and anthocyanin content (C) in the skin of un-bagged ('Control') and bagged ('Bagged') 'Apple' mango. Fruit were bagged using brown paper bags at 60 days after full bloom in Kaiti. X-axis scale in days after harvest (DAH). Data represent means ± se of 12 to 16 (A) and 3 (B, C) fruit.

ethylene synthesis, which increased with time, reached a peak at about 4 and 8 DAH in the un-bagged control and the bagged fruit, respectively, and decreased thereafter. The peak in ethylene synthesis was about two-fold higher in the un-bagged control than in the bagged fruit (Fig. 6).

Titratable acidity (TA) decreased, whereas total soluble sugars (TSS) increased with shelf life. There was no difference between un-bagged control and bagged fruit (Fig. 7). There were also no differences in firmness, sucrose, glucose, fructose, vitamin C or calcium contents between bagged and un-bagged control fruit (Supplementary Figs. S2–4 and supplementary Table S1).

4. Discussion

Bagging improved pre- and postharvest performances of 'Apple' mango by i) reducing lenticel cracking and russeting, and ii) by decreasing postharvest water loss.

4.1. Bagged fruit had less lenticel cracking and was less russeted than un-bagged control fruit

Bagging reduced lenticel cracking as indexed by lenticels with smaller core and pore areas. In 'Apple' mango, lenticels are sites where russet is initiated (Athoo et al., 2020). From a materials science point of view, lenticels represent stiffer areas in a larger area of less-stiff (more extensible) cuticle. Lenticels therefore tend to concentrate stresses (Brown and Considine, 1982; Considine, 1982) and this increases susceptibility to cracking (Athoo et al., 2021, 2023). In mango cv. 'Apple', the lenticels would seem to be far more susceptible to microcracking

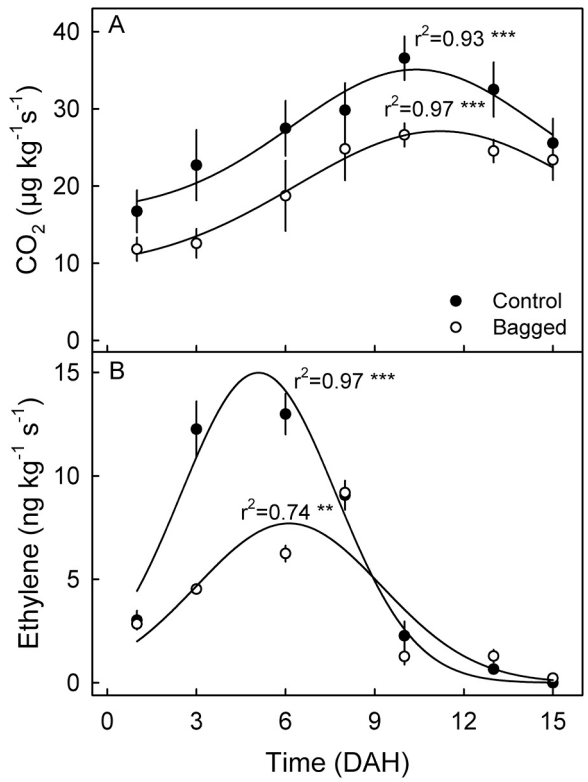

Fig. 6. Rates of respiration and ethylene release from mature bagged ('Bagged') and un-bagged ('Control') 'Apple' mango. The fruit were bagged using brown paper bags at 60 days after full bloom in Kaiti. X-axis scale in days after harvest (DAH). Data represent means ± se of three to six fruit.

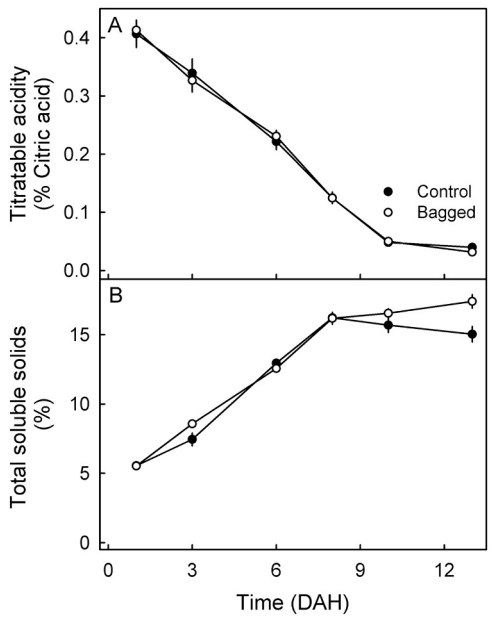

Fig. 7. Titratable acidity (TA) (A) and total soluble solids (TSS) (B) of the pulp of mature bagged ('Bagged') and un-bagged ('Control') 'Apple' mango. The fruit were bagged using brown paper bags (Blue star®) at 60 days after full bloom at Kaiti. X-axis scale in days after harvest (DAH). Data represent means ± se of 15 fruit.

than those in other mango cultivars (Athoo et al., 2021, 2023). Our finding that lenticels serve as initiation points for microcracking is consistent with reports for other fruit crop species including for pear (Amarante et al., 2002) and pomegranate (Sarkomi et al., 2019). Our bagged 'Apple' mango fruit also suffered less microcracking around the lenticels and also less microcracking on the intervening fruit surface, so the fruit were almost russet-free.

The reduction in lenticel cracking and the decrease in russeting in the bagged fruit would seem to be the result of reduced surface wetness in bagged fruit. Surface wetness has previously been shown to trigger microcracking in 'Apple' mango (Athoo et al., 2022), sweet cherry (Knoche and Peschel, 2006), grape berry (Becker and Knoche., 2012) and *Malus* apple (Tukey, 1969; Knoche and Grimm, 2008; Chen et al., 2020; Khanal et al., 2020). Exposure to surface moisture alters the rheological properties of the strained cuticle and this increases the likelihood of failure (Khanal and Knoche, 2017). Earlier data established that the deposition rate of cuticle is low in 'Apple' mango and that this increases elastic strain, weakens the cuticle, and increases microcracking (Athoo et al., 2021). Microcracking of the cuticle is the first visual symptom in russeting in susceptible species and cultivars (Athoo et al., 2021; Faust and Shear, 1972; Chen et al., 2020).

It is interesting that the CM, DCM and wax mass were all significantly lower in the bagged fruit, compared with the un-bagged controls. The bags probably acted as a transpiration barrier due to the resistance of the bag itself arranged in series to the cuticle plus the boundary layer resistance of the still air inside the bag. Both factors reduce transpiration. Lower transpiration inside the bags may have suppressed CM deposition (Skoss, 1955; Hao et al., 2011). Suppressed CM deposition has been reported in shaded compared to sun-exposed mango (Léchaudel et al., 2013) or grape berries (Rosenquist and Morrison, 1989). Our findings are consistent with effects of bagging on CM deposition in pear and persimmon (Amarante et al., 2002; Katagiri et al., 2003).

4.2. *Bagging improved postharvest performance in 'Apple' mango*

Bagging improved postharvest performance. First, bagged fruit maintained a more intact cuticle barrier that is effective in restricting transpiration and in pathogen defense. In fact, bagging has been reported to reduce the incidence of anthracnose and stem end rot in 'Nam Dok Mai #4′ and 'Keitt' mango (Hofman et al., 1997; Chonhenchob et al., 2011). Similar findings have been reported for pear, pummelo, papaya etc. (Kitagawa et al., 1992; Issarakraisila, 2018; Gao et al., 2022). Second, bagged fruit had lower postharvest water loss than un-bagged control fruit. Non-russeted fruit surfaces have a lower permeance than russeted surfaces in 'Apple' mango (Athoo et al., 2020) and *Malus* apple (Khanal et al., 2019). Third, bagging increased peel quality in 'Apple' mango and many other fruit crops e.g., pear (Amarante et al., 2002). Fruit appearance was improved by reduced russeting. The ground color was not affected by bagging, as indicated by the hue angle of the peel. There was no change in carotenoid content, this is in line with earlier studies in other mango cultivars (Hofman et al., 1997; Ding and Syakirah, 2010). That bagging decreased the red blush and reduced anthocyanin content compared with un-bagged control fruit, is not unique to 'Apple' mango, but has also been reported for bagged *Malus* apple (Chen et al., 2012), peach (Jia et al., 2005), and pomegranate (Sarkomi et al., 2019). See Ali et al. (2021) for a detailed review. Reduced anthocyanin content is common in shaded compared to sun-exposed fruit (Bible and Singha, 1993; Karanjalker et al., 2018). This is due to the reduced exposure to UV light in bagged fruit – UV is required for anthocyanin synthesis (Ubi et al., 2006; Karanjalker et al., 2018). We show that brown paper bags absorb light in the UV wavelength range.

We detected no adverse effects of bagging on fruit quality. Organic acids, sugars, vitamin C and Ca were largely unaffected. The lack of an effect of bagging on Ca content is consistent with earlier studies in 'Kensington Pride', 'Sensation' and 'Keitt' mango (Hofman et al., 1997; Joyce et al., 1997; Beasley et al., 1999).

5. Conclusion

The results presented here indicate that preharvest bagging is a commercially attractive procedure able to reduce russeting in 'Apple' mango. In addition, bagged fruit were larger and suffered lower post-harvest weight loss than un-bagged control fruit. Except for a reduced blush, there were no adverse effects of bagging on fruit quality or nutritional value. Thus, pre-harvest bagging offers an opportunity for small-scale farmers to produce high quality 'Apple' mangos suitable for discerning export markets.

Funding

The study was funded by a grant (KN 402/21-1) from the Deutsche Forschungsgemein-schaft.

CRediT authorship contribution statement

Athoo Thomas O.: Writing – review & editing, Writing – original draft, Visualization, Validation, Methodology, Investigation, Formal analysis, Data curation. **Knoche Moritz:** Writing – review & editing, Writing – original draft, Visualization, Validation, Supervision, Resources, Project administration, Methodology, Funding acquisition, Formal analysis, Data curation, Conceptualization. **Yegon Dennis:** Investigation, Formal analysis. **Owino Willis O.:** Writing – review & editing, Writing – original draft, Validation, Supervision, Resources, Project administration.

Declaration of Competing Interest

The authors declare that they have no known competing financial interests or personal relationships that could have appeared to influence the work reported in this paper.

Data availability

Data will be made available on request.

Acknowledgements

We thank Mr. Julius Waweru and Mrs. Jane Kathuli for letting us use their mango orchards, Dr. Andreas Winkler, Simon Sitzenstock, Rachel Mwendwa and David Abuga for technical support and Dr. Sandy Lang for thoughtful comments on this manuscript.

Appendix A. Supporting information

Supplementary data associated with this article can be found in the online version at doi:10.1016/j.postharvbio.2024.112804.

References

Ali, M.M., Anwar, R., Yousef, A.F., Li, B., Luvisi, A., De Bellis, L., Aprile, A., Chen, F., 2021. Influence of bagging on the development and quality of fruits. Plants 10 (2), 358. https://doi.org/10.3390/plants10020358.

Amarante, C., Banks, N.H., Max, S., 2002. Preharvest bagging improves packout and fruit quality of pears (*Pyrus communis*). N. Z. J. Crop Hortic. Sci. 30, 93–98. https://doi.org/10.1080/01140671.2002.9514203.

Athoo, T., Winkler, A., Owino, W.O., Knoche, M., 2023. Lenticels are sites of initiation of microcracking and russeting in 'Apple' mango. Plos One 18 (9), e0291129. https://doi.org/10.1371/journal.pone.0291129.

Athoo, T.O., Winkler, A., Knoche, M., 2020. Russeting in 'Apple' mango: Triggers and mechanisms. Plants 9, 898. https://doi.org/10.3390/plants9070898.

Athoo, T.O., Khanal, B.P., Knoche, M., 2021. Low cuticle deposition rate in 'Apple' mango increases elastic strain, weakens the cuticle and increases russet. PLoS One 16, 1–19. https://doi.org/10.1371/journal.pone.0258521.

Athoo, T.O., Winkler, A., Owino, W.O., Knoche, M., 2022. Surface moisture induces microcracks and increases water vapor permeance of fruit skins of mango cv. Apple. Horticulturae 8, 545. https://doi.org/10.3390/horticulturae8060545.

Beasley, D.R., Joyce, D.C., Hofman, P.J., 1999. Effect of preharvest bagging and of embryo abortion on calcium levels in 'Kensington Pride' mango fruit. Austr. J. Exp. Agric. 39, 345. https://doi.org/10.1071/EA98060.

Becker, T., Knoche, M., 2012. Water induces microcracks in the grape berry cuticle. Vitis J. Grapevine Res 51, 141–142. https://doi.org/10.15488/3851.

Bible, B.B., Singha, S., 1993. Canopy position influences CIELAB coordinates of peach color. HortScience 28, 992–993. https://doi.org/10.21273/HORTSCI.28.10.992.

Brown, K., Considine, J., 1982. Physical aspects of fruit growth stress distribution around lenticels. Plant Physiol. 69, 585–590. https://doi.org/10.1104/pp.69.3.585.

Burdon, I.N., Moore, K.G., Wainwright, H., 1991. Mineral distribution in mango fruit susceptible to the physiological disorder soft-nose. Sci. Hortic. 48, 329–336. https://doi.org/10.1016/0304-4238(91)90143-M.

Chen, C.S., Zhang, D., Wang, Y.Q., Li, P.M., Ma, F.W., 2012. Effects of fruit bagging on the contents of phenolic compounds in the peel and flesh of 'Golden Delicious', 'Red Delicious', and 'Royal Gala' apples. Sci. Hortic. 142, 68–73. https://doi.org/10.1016/J.SCIENTA.2012.05.001.

Chen, Y.H., Straube, J., Khanal, B.P., Knoche, M., Debener, T., 2020. Russeting in apple is initiated after exposure to moisture ends—i. Histological evidence. Plants 9, 1–18. https://doi.org/10.3390/plants9101293.

Chonhenchob, V., Kamhangwong, D., Kruenate, J., Khongrat, K., Tangchantra, N., Wichai, U., Singh, S.P., 2011. Preharvest bagging with wavelength-selective materials enhances development and quality of mango (*Mangifera indica* L.) cv. Nam Dok Mai #4. J. Sci. Food Agric. 91, 664–671. https://doi.org/10.1002/jsfa.4231.

Cohen, H., Dong, Y., Szymanski, J., Lashbrooke, J., Meir, S., Almekias-Siegl, E., Zeisler-Diehl, V.V., Schreiber, L., Aharoni, A., 2019. A multilevel study of melon fruit reticulation provides insight into skin ligno-suberization hallmarks. Plant Physiol. 179, 1486–1501. https://doi.org/10.1104/pp.18.01158.

Considine, J.A., 1982. Physical aspects of fruit growth: cuticular fracture and fracture patterns in relation to fruit structure in *Vitis vinifera*. J. Hortic. Sci. 57, 79–91. https://doi.org/10.1080/00221589.1982.11515027.

Ding, P., Syakirah, M.N., 2010. Influence of fruit bagging on postharvest quality of 'Harumanis' mango (*Mangifera indica* L.). Acta Hortic. (877), 169–174. https://doi.org/10.17660/ActaHortic.2010.877.15.

Edelmann, H.G., Neinhuis, C., Bargel, H., 2005. Influence of hydration and temperature on the rheological properties of plant cuticles and their impact on plant organ integrity. J. Plant Growth Regul. 24, 116–126. https://doi.org/10.1007/s00344-004-0015-5.

Evert, R.F., 2006. Esau's plant anatomy. John Wiley & Sons, Inc., Hoboken, NJ, USA https://doi.org/10.1002/0470047380.

Faust, M., Shear, C.B., 1972. Russeting of apples, an interpretive review. HortScience 7, 233–235.

Gao, C., Zhang, Y., Li, H., Gao, Q., Cheng, Y., Ogunyemi, S.O., Guan, J., 2022. Fruit bagging reduces the postharvest decay and alters the diversity of fruit surface fungal community in 'Yali' pear. BMC Microbiol 22, 239. https://doi.org/10.1186/s12866-022-02653-4.

Geyer, U., Schönherr, J., 1988. In vitro test for effects of surfactants and formulations on permeability of plant cuticles, in: Cross, B. and Scher, H.B. (Ed.), Pesticide Formulations: Innovations and Developments. Washington, DC, USA, pp. 22–33. https://doi.org/10.1021/bk-1988–0371.ch003.

Hao, Y., Zhao, Q., Liu, Q., Li, W., 2011. Effects of the micro-environment inside fruit bags on the structure of fruit peel in 'Fuji' apple. Shengtai Xuebao/ Acta Ecol. Sin. 31, 2831–2836.

Heinonen, M.I., 1990. Carotenoids and provitamin A activity of carrot (*Daucus carota* L.) cultivars. J. Agric. Food Chem. 38, 609–612. https://doi.org/10.1021/jf00093a005.

Hofman, P.J., Smith, L.G., Joyce, D.C., Johnson, G.I., Meiburg, G.F., 1997. Bagging of mango (*Mangifera indica* cv. 'Keitt') fruit influences fruit quality and mineral composition. Postharvest Biol. Technol. 12, 83–91. https://doi.org/10.1016/S0925-5214(97)00039-2.

Isaac, R.A., Johnson, W.C., 1975. Collaborative study of wet and dry ashing techniques for the elemental analysis of plant tissue by atomic absorption spectrophotometry. J. AOAC Int. 58, 436–440. https://doi.org/10.1093/jaoac/58.3.436.

ISO, 1998. ISO 750:1998 Fruit and vegetable products — Determination of titratable acidity, 2nd ed. International Organization for Standardization (ISO), Geneva, Switzerland.

Issarakraisila, M., 2018. Effect of types of bagging materials on growth, quality and disease-insect damages in pummelo fruit in tropical humid conditions. Acta Hortic. (1208), 319–323. https://doi.org/10.17660/ActaHortic.2018.1208.43.

Jia, H.J., Araki, A., Okamoto, G., 2005. Influence of fruit bagging on aroma volatiles and skin coloration of 'Hakuho' peach (*Prunus persica* Batsch). Postharvest Biol. Technol. 35, 61–68. https://doi.org/10.1016/j.postharvbio.2004.06.004.

Joyce, D.C., Beasley, D.R., Shorter, A.J., 1997. Effect of preharvest bagging on fruit calcium levels, and storage and ripening characteristics of 'Sensation' mangoes. Austr. J. Exp. Agric. 37, 383. https://doi.org/10.1071/EA96074.

Karanjalker, G.R., Ravishankar, K.V., Shivashankara, K.S., Dinesh, M.R., 2018. Influence of bagging on color, anthocyanin and anthocyanin biosynthetic genes in peel of red colored mango cv. 'Lily. Erwerbs Obstbau 60, 281–287. https://doi.org/10.1007/s10341-018-0371-0.

Katagiri, T., Satoh, Y., Fukuda, T., Kataoka, I., 2003. Improving marketability of "Fuyu" persimmon fruit by bagging culture. Acta Hortic. (601), 213–217. https://doi.org/10.17660/ActaHortic.2003.601.30.

Khanal, B.P., Knoche, M., 2014. Mechanical properties of apple skin are determined by epidermis and hypodermis. J. Am. Soc. Hortic. Sci. 139, 139–147. https://doi.org/10.21273/jashs.139.2.139.

Khanal, B.P., Knoche, M., 2017. Mechanical properties of cuticles and their primary determinants. J. Exp. Bot. 68, 5351–5367. https://doi.org/10.1093/jxb/erx265.

Khanal, B.P., Ikigu, G.M., Knoche, M., 2019. Russeting partially restores apple skin permeability to water vapour. Planta 249, 849–860. https://doi.org/10.1007/s00425-018-3044-1.

Khanal, B.P., Imoro, Y., Chen, Y.H., Straube, J., Knoche, M., 2020. Surface moisture increases microcracking and water vapour permeance of apple fruit skin, 1–9 Plant Biol.. https://doi.org/10.1111/plb.13178.

Kitagawa, H., Manabe, K., Esguerra, E.B., 1992. Bagging of fruit on the tree to control disease. Acta Hortic. 321, 871–875. https://doi.org/10.17660/ActaHortic.1992.321.110.

Knoche, M., Grimm, E., 2008. Surface moisture induces microcracks in the cuticle of 'Golden Delicious' apple. HortScience 43, 1929–1931. https://doi.org/10.21273/hortsci.43.6.1929.

Knoche, M., Lang, A., 2017. Ongoing growth challenges fruit skin integrity. CRC Crit. Rev. Plant Sci. 36, 190–215. https://doi.org/10.1080/07352689.2017.1369333.

Knoche, M., Peschel, S., 2006. Water on the surface aggravates microscopic cracking of the sweet cherry fruit cuticle. J. Am. Soc. Hortic. Sci. 131, 192–200. https://doi.org/10.21273/jashs.131.2.192.

Knoche, M., Peschel, S., Hinz, M., Bukovac, M.J., 2000. Studies on water transport through the sweet cherry fruit surface: characterizing conductance of the cuticular membrane using pericarp segments. Planta 212, 127–135. https://doi.org/10.1007/s004250000404.

Léchaudel, M., Lopez-Lauri, F., Vidal, V., Sallanon, H., Joas, J., 2013. Response of the physiological parameters of mango fruit (transpiration, water relations and antioxidant system) to its light and temperature environment. J. Plant Physiol. 170, 567–576. https://doi.org/10.1016/J.JPLPH.2012.11.009.

Lee, J., Durst, R.W., Wrolstad, R.E., Barnes, K.W., Eisele, T., Giusti, M.M., Haché, J., Hofsommer, H., Koswig, S., Krueger, D.A., Kupina, S., Martin, S.K., Martinsen, B.K., Miller, T.C., Paquette, F., Ryabkova, A., Skrede, G., Trenn, U., Wightman, J.D., 2005. Determination of total monomeric anthocyanin pigment content of fruit juices, beverages, natural colorants, and wines by the pH differential method: collaborative study. J. AOAC Int. 88, 1269–1278.

Li, B.W., 1996. Determination of sugars, starches, and total dietary fiber in selected high-consumption foods. J. AOAC Int. 79, 718–723. https://doi.org/10.1093/jaoac/79.3.718.

Lin, J., Chang, Y., Yan, Z., Li, X., 2008. Effects of bagging on the quality of pear fruit and pesticide residues. Acta Hortic. 772, 315–318. https://doi.org/10.17660/actahortic.2008.772.52.

Ma, X., Liu, B., Zhang, Y., Su, M., Zheng, B., Wang, S., Wu, H., 2023. Unraveling correlations between calcium deficiency and spongy tissue in mango fruit flesh. Sci. Hortic. 309, 111694 https://doi.org/10.1016/j.scienta.2022.111694.

Mathooko, F.M., Kahangi, E.M., Runkua, J.M., Onyango, C.A., Owino, W.O., 2011. Preharvest mango (*Mangifera indica* L. 'Apple') fruit bagging controls lenticel discolouration and improves postharvest quality. Acta Hortic. (906), 55–62. https://doi.org/10.17660/ActaHortic.2011.906.7.

McGuire, R.G., 1992. Reporting of objective color measurements. HortScience 27, 1254–1255. https://doi.org/10.21273/hortsci.27.12.1254.

Michailides, T.J., 1991. Russeting and russet scab of prune, an environmentally induced fruit disorder: symptomatology, induction, and control. Plant Dis. 75, 1114. https://doi.org/10.1094/PD-75-1114.

Moon, Y.J., Nam, K.W., Kang, I.K., Moon, B.W., 2016. Effects of tree-spray of calcium agent, coating agent, $GA4_{+7}$ + BA and paper bagging on russet prevention and quality of 'Gamhong' apple fruits. Hortic. Sci. Technol. 34, 528–536. https://doi.org/10.12972/kjhst.20160054.

Nobel, P.S., 2020. Physicochemical and Environmental Plant Physiology, fifth ed..,. Academic Press, San Diego, California.

Orgell, W.H., 1955. The isolation of plant cuticle with pectic enzymes. Plant Physiol. 30, 78–80. https://doi.org/10.1104/pp.30.1.78.

Osborne, D.R., Voogt, P., 1978. The Analysis of Nutrients in Foods. Academic Press Inc, London.

Peschel, S., Knoche, M., 2005. Characterization of microcracks in the cuticle of developing sweet cherry fruit. J. Am. Soc. Hortic. Sci. 130, 487–495. https://doi.org/10.21273/JASHS.130.4.487.

Rodriguez-Amaya, D.B., Kimura, M., 2004. Handbook for carotenoid analysis. International Food Policy Research Institute (IFPRI), Washington, DC.

Rosenquist, J.K., Morrison, J.C., 1989. Some factors affecting cuticle and wax accumulation on grape berries. Am. J. Enol. Vitic. 40, 241–244. https://doi.org/10.5344/ajev.1989.40.4.241.

Sarkomi, F.H., Moradinezhad, F., Khayat, M., 2019. Pre-harvest bagging influences sunburn, cracking and quality of pomegranate fruits. J. Hortic. Postharvest Res. 2, 131–142. https://doi.org/10.22077/jhpr.

Shi, C., Qi, B., Wang, X., Shen, L., Luo, J., Zhang, Y., 2019. Proteomic analysis of the key mechanism of exocarp russet pigmentation of semi-russet pear under rainwater condition. Sci. Hortic. 254, 178–186. https://doi.org/10.1016/j.scienta.2019.04.086.

Si, Y., Khanal, B.P., Schlüter, O.K., Knoche, M., 2021. Direct evidence for a radial gradient in age of the apple fruit cuticle. Front. Plant Sci. 12, 1–12. https://doi.org/10.3389/fpls.2021.730837.

Skene, D.S., 1982. The development of russet, rough russet and cracks on the fruit of the apple Cox's Orange Pippin during the course of the season. J. Hortic. Sci. 57, 165–174. https://doi.org/10.1080/00221589.1982.11515037.

Skoss, J.D., 1955. Structure and composition of plant cuticle in relation to environmental factors and permeability. Bot. Gaz. 117, 55–72. https://doi.org/10.1086/335891.

Tukey, L.D., 1969. Observations on the russeting of apples growing in plastic bags. Proc. Amer. Soc. Hortic. Sci. 74, 30–39.

Ubi, B.E., Honda, C., Bessho, H., Kondo, S., Wada, M., Kobayashi, S., Moriguchi, T., 2006. Expression analysis of anthocyanin biosynthetic genes in apple skin: effect of UV-B and temperature. Plant Sci. 170, 571–578. https://doi.org/10.1016/j.plantsci.2005.10.009.

Vikram, V.B., Ramesh, M.N., Prapulla, S.G., 2005. Thermal degradation kinetics of nutrients in orange juice heated by electromagnetic and conventional methods. J. Food Eng. 69, 31–40. https://doi.org/10.1016/j.jfoodeng.2004.07.013.

Wexler, A., 1995. Constant humidity solutions. Handbook of Chemistry and Physics, seventy sixth ed.,. CRC Press, Boca Raton, FL.

Winkler, A., Athoo, T., Knoche, M., 2022. Russeting of fruits: etiology and management. Horticulturae 8, 231. https://doi.org/10.3390/horticulturae8030231.

Yuan, G., Bian, S., Han, X., He, S., Liu, K., Zhang, C., Cong, P., 2019. An integrated transcriptome and proteome analysis reveals new insights into russeting of bagging and non-bagging 'Golden Delicious' apple. Int. J. Mol. Sci. 20, 4462. https://doi.org/10.3390/ijms20184462.